SCIENTIFIC REPORTS

OPEN

SUBJECT AREAS:
ADHERENS JUNCTIONS
ENDOCYTOSIS

Received
31 July 2013

Accepted
20 September 2013

Published
7 October 2013

Correspondence and requests for materials should be addressed to M.P. (maddy.parsons@kcl.ac.uk)

* These authors contributed equally to this work.

CAR regulates epithelial cell junction stability through control of E-cadherin trafficking

Penny E. Morton[1,2], Alexander Hicks[1], Theodoros Nastos[1], George Santis[1]* & Maddy Parsons[2]*

[1]Division of Asthma, Allergy & Lung Biology, King's College London, 5th Floor Tower Wing, Guy's Hospital Campus, London, United Kingdom, [2]Randall Division of Cell and Molecular Biophysics, King's College London, New Hunt's House, Guys Campus, London, United Kingdom.

CAR (Coxsackie and Adenovirus Receptor) is the primary docking receptor for typeB coxsackie viruses and subgroup C adenoviruses. CAR is a member of the JAM family of adhesion receptors and is located to both tight and adherens junctions between epithelial cells where it can assemble adhesive contacts through homodimerisation *in trans*. However, the role of CAR in controlling epithelial junction dynamics remains poorly understood. Here we demonstrate that levels of CAR in human epithelial cells play a key role in determining epithelial cell adhesion through control of E-cadherin stability at cell-cell junctions. Mechanistically, we show that CAR is phosphorylated within the C-terminus by PKCδ and that this in turn controls Src-dependent endocytosis of E-cadherin at cell junctions. This data demonstrates a novel role for CAR in regulating epithelial homeostasis.

Dynamic control of epithelial cell-cell junctions is vital to many biological processes including embryonic development, tissue homeostasis, wound healing and inflammation. Incorrect control of epithelial cell-cell junctions has been implicated in many disease processes, including cancer. The integrity of epithelial junctions is maintained by families of transmembrane receptors whose inter-cellular homo- or hetero-dimerisation form and maintains cell-cell contacts. Control of these adhesions is then mediated by extracellular factors, endocytosis/exocytosis of the receptors and interactions with cytoplasmic binding partners including the cytoskeleton[1].

One such cell adhesion protein is the coxsackie and adenovirus receptor (CAR) which is a member of the Junctional Adhesion Molecule (JAM) family of junctional adhesion molecules, as well as a viral receptor for type B coxsackievirus and subgroup C adenovirus[2]. The role of CAR in adenovirus infection has been well studied; however its role in cell adhesion and tissue homeostasis is not well understood. CAR has been shown to localise to both tight and adherens junctions in different epithelial cell types, and to co-precipitate with tight junction proteins in MDCK cells[3] and endothelial cells[4] suggesting that it has a role in formation and/or maintenance of tight junctions. However recent studies have highlighted tissue specific roles as CAR knockout mice have defects in vascular permeability in the lymphatic system[5] and in heart muscle[6], but tight junctions in the intestine are unaffected by the loss of CAR[6]. The role of CAR in other epithelial types, for example respiratory epithelium, has not been well studied despite the gross changes in lung morphology observed in CAR knockout mice[6]. Our own previous work has shown that CAR expression levels affect recruitment of adherens junction proteins in MCF-7 human breast carcinoma cells without affecting basal paracellular permeability[7]. Moreover, CAR expression has been shown to correlate with tumour progression in some types of epithelial-derived cancer including lung cancers and in some cases to specifically correlate with reduced E-cadherin expression, a marker for EMT[8–11]. These data suggest CAR can play important tissue specific roles in the control of cell-cell adhesion.

Our previous studies have shown that high levels of CAR can affect recruitment of E-cadherin to cell-cell contacts in MCF-7 cells[7]. However how CAR controls localisation of E-cadherin, whether this effect is specific to E-cadherin and the functional consequences of this are unknown. E-cadherin localisation to junctions can be controlled through a number of different mechanisms[12]. At cell-cell contacts E-cadherin forms calcium dependent homodimers in trans with opposing E-cadherin molecules on neighbouring cells. Stabilisation of E-cadherin is in part controlled by interaction to cytoplasmic adaptor proteins; β-catenin and p120-catenin. β-catenin binds to E-cadherin soon after transcription and facilitates trafficking of E-cadherin to the cell membrane. Whereas p120-catenin is thought to join this complex at or adjacent to the membrane and inhibit endocytosis, in addition

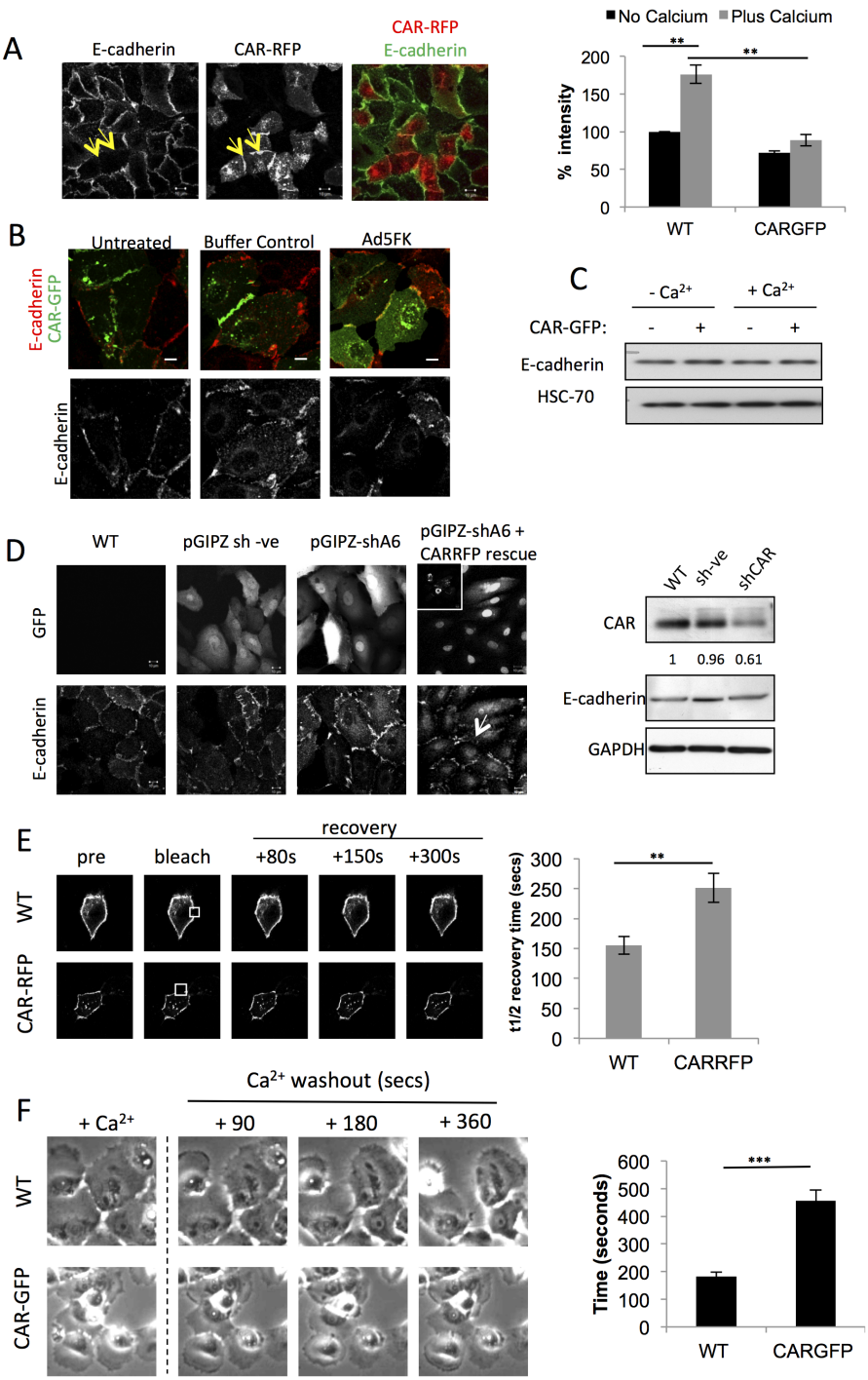

Figure 1 | CAR mediates E-cadherin localisation to epithelial cell junctions and mediates junction stability. (A) Confocal microscopy of E-cadherin localisation in a 50 : 50 mix of WT and CARRFP HBEC. Arrows highlight loss of E-cadherin at CARRFP positive junctions (left), quantification of E-cadherin intensity in monolayers of WT or CARGFP HBEC by wide-field microscopy, with and without calcium (right). (B) Confocal microscopy of E-cadherin localisation in a 50 : 50 mix of WT and CARGFP HBEC, in untreated, buffer alone control and Ad5FK treated cells. Colocalisation of E-cadherin and CARGFP in the presence of Ad5FK is pseudo-coloured yellow. (C) Western blot analysis of wild-type and CAR-GFP HBEC in the presence or absence of calcium probed for E-cadherin and HSC-70. (D) Confocal microscopy of E-cadherin localisation in WT, control shRNA expressing, CAR shRNA expressing HBEC and CAR shRNA HBEC expressing sh-resistant CAR-RFP(arrow highlights and sh-resistant CAR-RFP expressing cell-cell junctions showing reduced E-cadherin). Western blot showing CAR and E-cadherin expression in WT HBEC or HBEC expressing control shRNA or shRNA directed at CAR (right). (E) Quantification of FRAP recovery data of E-cadherin-GFP expressed in wild-type or CAR-RFP HBEC. Histogram shows t1/2 recovery time for E-cadherin-GFP at junctions in wild-type HBEC (n = 18) and CAR-RFP HBEC (n = 15). (F) Dissociation of cell-cell contacts in wild-type and CAR GFP HBEC cells upon removal of calcium. Images show phase contrast of wild-type or CAR-GFP HBEC grown in calcium containing media, before and after the media was replaced with calcium free media (for times indicated). Graph shows analysis of junction dissolution quantified as the average time taken for individual cell-cell junctions to dissociate. Data is the mean of at least 100 junctions per data set. Error bars are SEM. * = $p < 0.05$, ** = $p < 0.01$ *** = $p < 0.005$. Scale bars correspond to 10 μm.

to promoting exocytosis of E-cadherin (reviewed in[13,14]. Recent studies using fluorescence recovery after photobleaching (FRAP) to study dynamics of E-cadherin-GFP in mature junctions showed that rather than being static, the majority of E-cadherin is being dynamically endocytosed and recycled suggesting that control of E-cadherin trafficking is essential to maintenance of epithelial layers[15].

E-cadherin endocytosis has been shown to occur via clathrin-dependent and independent, pathways, caveolin-dependent mechanisms and a macropinocytosis pathway[14,16–18]. Removal of E-cadherin from cell-cell adhesions through these pathways can either lead to degradation or recycling of the receptor back to the membrane, and ultimately the local regulation of cell-cell adhesion. Previous studies have also shown that the non-receptor tyrosine kinase Src controls E-cadherin endocytosis through either a coat-mediated internalisation[19], or macropinocytosis[20,21]. In addition the protein kinase C (PKC) family of kinases are known to be involved in the endocytosis of E-cadherin[16]. Recently, PKCδ has been shown to promote internalisation of E-cadherin and dissolution of cell junctions, suggesting an important role for this kinase in the control of E-cadherin internalisation[22].

In this study we aimed to understand the mechanism by which CAR regulates E-cadherin levels at cell-cell contacts. Our data demonstrates that high levels of CAR destabilises Ecadherin at cell junctions to promote endocytosis of E-cadherin through different recycling pathways. We further show that phosphorylation of the cytoplasmic domain of CAR by PKCδ is a key regulatory point in controlling E-cadherin stability. These data highlight CAR as a key molecular player in the regulation of epithelial junctional homeostasis.

Results

CAR expression levels control E-cadherin localisation to cell-cell junctions. CAR has previously been shown to localise to tight junctions (TJ)[3,4]. However, CAR knock-out mice do not show defects in TJ in all epithelial tissues suggesting the role of CAR may differ between cell and tissue types[6]. Indeed we have recently shown that CAR can modulate recruitment of adherens junction proteins[7] suggesting CAR may also control epithelial homeostasis through adherens junctions. We therefore analysed the effects of stable CAR-FP expression on junction stability in human bronchial epithelial cells (HBEC), which express very low levels of endogenous CAR. CAR-GFP expression had no basal effect on paracellular permeability (Fig. S1A) or recruitment of tight junction proteins to cell-cell contacts (Fig. S2A, B). This suggests that CAR may not have a major role in tight junction formation or maintenance in bronchial epithelial cells. As our previous data have suggested a regulatory link between junctional CAR and E-cadherin in MCF7 cells[7,23] we used E-cadherin as a marker to further define the effect of CAR on epithelial junction formation. 1 : 1 mixtures of control and CAR-RFP expressing HBEC (herein referred to as CAR-RFP HBEC) showed a dramatic reduction in localisation of E-cadherin at CAR-RFP positive cell junctions compared with neighbouring CAR-RFP negative junctions (Fig. 1A) in keeping with our previous observations in MCF7 cells[7]. Similar results were also seen in primary human bronchial epithelial cells transiently expressing CAR-GFP (Fig. S1C) suggesting this is not an artefact of immortalised cell lines. Quantitative analysis of wide-field fluorescence images of E-cadherin in control and CAR-GFP HBEC revealed that addition of high calcium to the growth medium did not result in the expected enhanced recruitment of E-cadherin at CAR-GFP contacts suggesting that CAR acts to restrict or inhibit E-cadherin recruitment (Fig. 1A right panel). Additionally, shRNA-mediated knockdown of CAR in HBEC resulted in increased E-cadherin localisation and this was rescued by re-expression of an shRNA-resistant form of CAR-RFP, further supporting a specific role for CAR in control of E-cadherin localisation (Fig. 1D). Importantly, overexpression or knockdown of CAR did not alter total expression levels of E-cadherin (Fig. 1C and D right panel) suggesting that regulation occurs at the level of recruitment to junctions and that E-cadherin displaced from cell junctions by CAR is not subsequently degraded. Furthermore, the effect of disrupting stable CAR-mediated cell-cell contacts using recombinant fibre knob domain of Adenovirus Type5 (Ad5FK) was quantitatively measured and revealed that loss of CAR-CAR interactions resulted in re-recruitment of E-cadherin to CAR-GFP positive cell-cell contacts (Percentage reduction in E-cadherin intensity in the presence of CARGFP; Untreated: 62.11% +/− 5.48 SEM, Buffer: 52.33% +/− 8.71 SEM, FK: −1.75% +/− 8.29 SEM) (Fig. 1B). This data demonstrates that CAR association *in trans* can directly control stability of E-cadherin at cell junctions.

To further investigate this process we examined the dynamics of E-cadherin-GFP at cell-cell contacts in HBEC and CAR-RFP-HBEC. Overexpression of E-cadherin-GFP forced some of this molecule to localise to cell-cell junctions in CAR-RFP-HBEC, which enabled us to track dynamics. However, of note, CAR-RFP and E-cadherin-GFP were localised within discrete domains of cell-cell junctions with very little overlap (Fig. 1A, B). FRAP analysis in these cells revealed that the rate of E-cadherin-GFP recovery to CAR-RFP junctions was significantly reduced compared with WT HBEC (Fig. 1E) and further suggests that CAR promotes endocytosis or restricts recruitment of E-cadherin at cell-cell contacts.

We next investigated the functional significance of this CAR:E-cadherin crosstalk by examining the stability of calcium mediated cell-cell contacts in live cells. Control and CAR-GFP HBEC were allowed to form colonies in calcium containing media and subjected to live imaging following calcium washout. Both cell lines maintained cell-cell contacts in the presence of calcium and dissociated these contacts following calcium washout (Fig. 1F and Supplementary movies 1,2). Cell dissociation was preceded by a visible contractile response and followed by an increase in cell polarisation and subsequent migration away from the colony. Analysis of the speed of cell-cell dissociation revealed that CAR-GFP positive junctions dissociated significantly slower than control cell junctions (Fig. 1F). High levels of CAR can therefore regulate calcium sensitive junctional stability either through CAR-dependent reduced E-cadherin localisation to junctions or through CAR homodimerisation. As CAR dimerisation in trans is not known to be calcium-dependent, increasing the number of CAR molecules likely results in both displacement of E-cadherin and junctions that are less reliant upon calcium for stability.

CAR mediates disruption of junctional E-cadherin through control of endocytosis. E-cadherin is known to undergo endocytosis and this is proposed to control levels and dynamics of this protein at junctions (reviewed in[14]). Analysis of time-lapse movies of CAR-RFP and E-cadherin-GFP revealed high levels of vesicular E-cadherin-GFP in CAR-RFP expressing cells during junction remodelling (Fig. 2A and Supp movie 3). To investigate whether CAR may mediate E-cadherin localisation through modulating endocytosis, we used a surface labelling antibody internalisation assay. E-cadherin antibodies (HECD-1) were incubated with cells for 60 minutes, followed by acid stripping to remove surface antibody, fixation and confocal analysis. Images demonstrated that E-cadherin-positive endosomes were much larger in CAR-GFP HBEC than in WT cells following 60 minutes of HECD-1 internalisation (Fig. 2B). To confirm this result using an alternative approach, we also investigated E-cadherin localisation in WT and CAR-GFP HBEC after calcium wash-out to promote junction dissociation and E-cadherin internalisation (as in Fig. 1F). Cell-cell contacts dissociated in both cell types, and triggered internalisation of E-cadherin, within 10 min of calcium removal. However in CAR-GFP HBEC, E-cadherin positive vesicles were

again significantly larger than those seen in WT HBEC, and were predominantly located within the peri-nuclear region (Fig. 2B).

To further investigate a potential involvement for CAR in endocytosis of E-cadherin we examined localisation of CAR-GFP following calcium washout. Surprisingly we observed a population of CAR that colocalised with internalised E-cadherin both in vesicles (upper left and right) and at dissociating junctions (lower left)) (Fig. 2C). Since CAR-GFP and E-cadherin did not visibly colocalise in stable cell-cell junctions under high calcium conditions (Fig. 1A, B) this suggests that CAR may associate with E-cadherin specifically during early endocytosis following junction instability. To test this further, we performed co-immunoprecipitation assays between CAR and E-cadherin under high and low calcium culture conditions. In agreement with the confocal images, we detected a complex between CAR and E-cadherin in cells under low calcium conditions, which was subsequently lost in the presence of calcium (Fig. 2D). This further suggests that CAR and E-cadherin are found in complex specifically when E-cadherin is not stably maintained at adherens junctions. Finally, we quantified and compared total levels of endocytosed E-cadherin in WT vs CAR-GFP HBEC and CAR- knockdown HBEC cells using the HECD-1 internalisation assay. We observed highest binding of the HECD-1 antibody to the surface of CAR-knockdown cells, less to WT cells and the lowest levels in CAR-GFP cells (Fig. S1D and Fig. 2E), which agrees with the different levels of E-cadherin membrane localisation in these cells. However, when internalised E-cadherin intensity was normalised against surface associated anti-

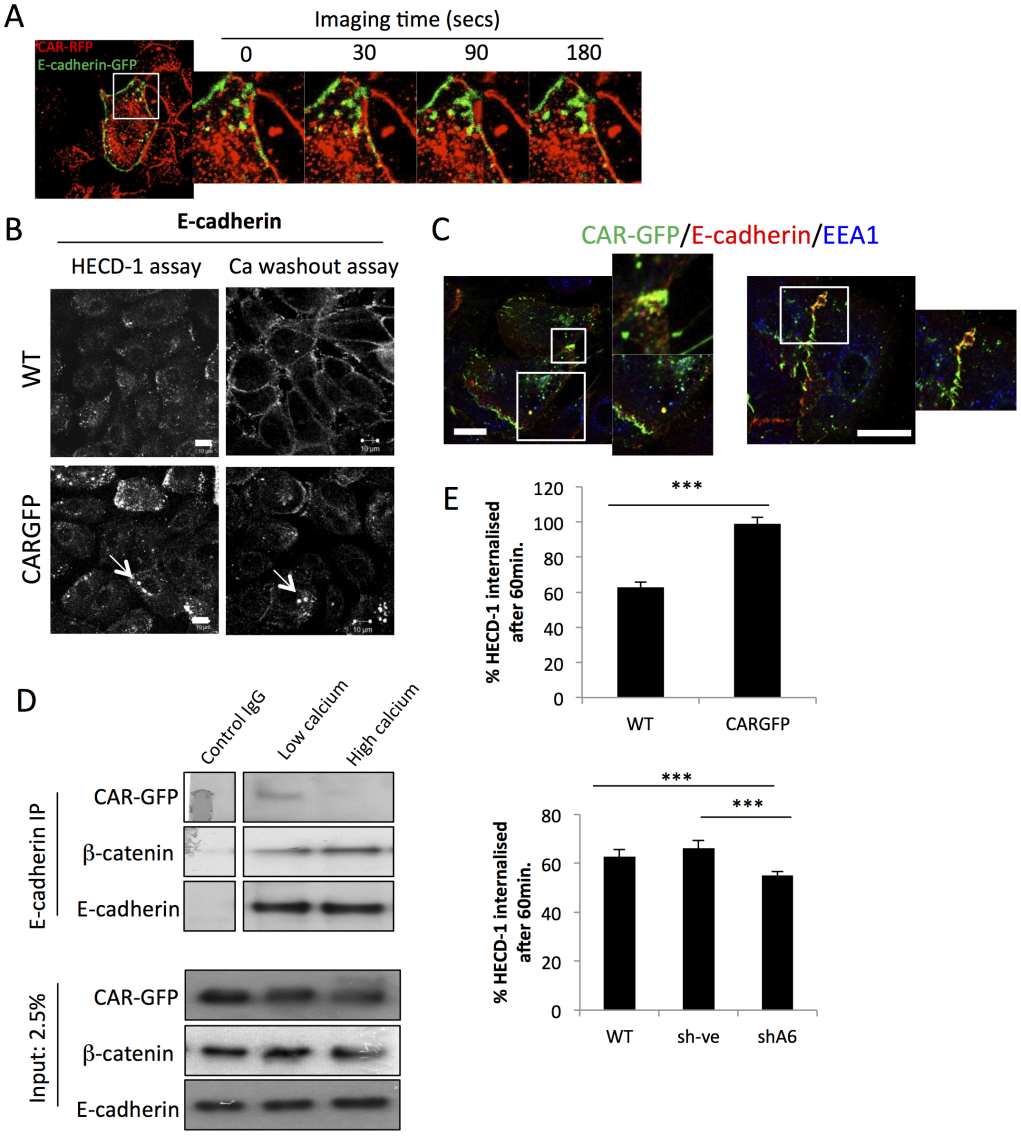

Figure 2 | CAR associates with E-cadherin to promote endocytosis. (A) Timelapse microscopy of HBEC expressing E-cadherin-GFP and CAR-RFP. Colocalisation is shown in yellow. (B) Confocal microscopy of internalised E-cadherin antibody (HECD-1) in antibody internalisation assay (left) and E-cadherin in calcium washout assay (right) in WT and CARGFP HBEC. Arrows point to large E-cadherin containing vesicles. (C) Confocal microscopy of CARGFP (green), E-cadherin (red) and EEA1 (blue) in vesicles (left and middle) and dissociating cell-cell junctions (right) in CARGFP HBEC. Colocalisation between CARGFP and E-cadherin is shown in yellow. (D) E-cadherin was immunoprecipitated from CAR-GFP-HBEC in the presence or absence of calcium. Immunoprecipitates were separated by SDS-PAGE and analysed by immunoblotting for E-cadherin, β-catenin and CARGFP. Control IP was performed in the absence of calcium. (E) Quantification of internalised HECD-1 (1 μg/ml) in WT vs CARGFP HBEC (top panel) and WT vs CAR knockdown (shA6) (bottom panel). More than 60 cells per condition were imaged using confocal microscopy to create Z-stacks of the whole cell. Maximum intensity projections of Z-stacks were exported to imageJ for intensity analysis. Internalised HECD-1 was normalised to bound HECD-1 to account for differences in antibody binding due to differences in E-cadherin membrane localisation. Error bars are SEM. * = $p < 0.05$, ** = $p < 0.01$ *** = $p < 0.005$. Scale bars correspond to 10 μm.

body in cells fixed prior to HECD-1 uptake, CARGFP cells showed significantly higher E-cadherin internalisation compared with WT cells (Fig. 2E, top panel). In addition, CAR-knockdown cells (shA6) showed a significant decrease in E-cadherin inernalisation compared with WT cells (Fig. 2E, bottom panel). Therefore, the levels and fate of internalised E-cadherin is altered in cells overexpressing CAR.

To investigate the nature of the E-cadherin positive vesicles in more detail, we analysed a time-course of E-cadherin internalisation in WT and CARGFP cells following incubation with HECD-1 (Fig. 3A). In WT HBEC we observed large numbers of small E-cadherin positive endosomes (average diameter 0.5 μm) that migrated to the perinuclear region of the cell over time (Fig. 3A, top panel). By contrast, CAR-GFP cells exhibited, large E-cadherin-positive circular structures (ranging in size from 1–5 μm) at early time-points that then accumulated within the perinuclear region over time (Fig. 3A). These were consistent in size and appearance with macropinosomes or late endosomal compartments[24]. Quantification of multiple images revealed a significant increase in the number of these structures in CAR-GFP HBEC compared with WT (Fig. 3B). E-cadherin can traffic via macropinocytosis in response to growth factor stimulation[18] and we therefore sought to investigate whether CAR might promote macropinocytosis of E-cadherin. To test this we performed HECD-1 internalisation assays in the presence or absence of a macropinocytosis inhibitor ethylisopropylamiloride (EIPA)[25]. Treatment with EIPA lead to reduced internalisation of HECD-1 and specifically reduced formation of macropinosome-like structures in both WT and CAR-GFP HBEC (Fig. 3C). In addition, EIPA treatment also led to increased junctional colocalisation between CAR-GFP and E-cadherin in mixtures of WT and CARGFP cells that was not seen under control conditions (Fig. 3D) suggesting that macropinocytosis is at least in part responsible for the effect of CAR overexpression on E-cadherin localisation. Indeed, these large E-cadherin positive vesicles showed partial colocalisation with two markers of macropinocytosis, Rabankyrin (Fig. 3F) and internalised dextran-Alexa597 (Fig. 3H). Interestingly, mixed cultures of WT and CAR-GFP HBEC treated with dynasore to inhibit dynamin-dependent endocytosis also exhibited increased E-cadherin at CAR positive cell-cell contacts and increased colocalisation between CAR-GFP and E-cadherin (Fig. 3E). Since dynamin is not required for macropinocytosis this data suggests that CAR does not specifically promote macropinocytosis of E-cadherin and may instead promote general endocytosis of E-cadherin through destabilisation of E-cadherin at cell junctions. In addition, the large E-cadherin-positive vesicles showed partial overlap with LAMP1 a marker of late endosomes and lysosomes (Fig. 3H). Moreover, we observed partial colocalisation between internalised HECD-1 and the late recycling endosome marker Rab7, within the peri-nuclear region of CAR-GFP HBEC (Fig. 3I). Since CAR-GFP expression does not promote degradation of E-cadherin (Fig. 1), colocalisation of internalised E-cadherin in CAR-GFP HBEC with LAMP1 and Rab7 most likely represents E-cadherin trafficking to late recycling endosomes rather than re-routing for degradation within lysosomes. Taken together these data demonstrate that CAR regulates E-cadherin localisation to cell-cell junctions by destabilising junctional E-cadherin and promoting E-cadherin internalisation through multiple internalisation routes.

CAR mediates endocytosis of E-cadherin through Src rather than through disruption of binding to catenins. Dynamics of E-cadherin at cell junctions are in part controlled through interactions with the cytoplasmic adaptor proteins β-catenin and p120catenin (reviewed in[26])[27]. To further probe the mechanism by which CAR controls E-cadherin stability, we performed confocal microscopy analysis to examine recruitment of β-catenin and p120-catenin to junctions in WT and CAR-GFP HBEC. Ectopic CAR expression significantly decreased recruitment of β-catenin to cell junctions (Fig. 4A) and also decreased junctional localisation of p120-catenin albeit to a lesser degree (Fig. 4B). Interestingly, junctional levels of the p120 catenin binding partner P-cadherin were higher in cells expressing CAR-RFP (Fig. S2D) importantly demonstrating that overexpressed CAR does not decrease junctional localisation of cell-cell adhesion proteins in general. Moreover, the tight junction associated protein ZO-1 localised similarly within WT and CAR-GFP positive cell-cell junctions showing that tight junction assembly is unaffected by overexpressed CAR (Fig. S2A and B). Expression of CAR-GFP did not alter complex formation between E-cadherin and either p120-catenin or β-catenin by co-immunoprecipitation (Fig. 4D). Disruption of E-cadherin binding to catenins is thought to destabilise junctional E-cadherin and promote endocytosis of E-cadherin. However β-catenin has also recently been shown to colocalise with E-cadherin on macropinosomes but not other early endosomes[18]. Consistently, we observed colocalisation between β-catenin and E-cadherin in large, macropinosome like vesicles in cells following HECD-1 antibody internalisation (Fig. 4E). This further suggests that CAR may act to promote macropinocytosis of E-cadherin without altering the balance of E-cadherin:catenin complex formation (Fig. 3D).

Src kinase has previously been shown to be involved in both dynamin-mediated endocytosis and macropinocytosis of E-cadherin[19,21]. To determine whether CAR might control E-cadherin dynamics through Src, we treated cells with PP2 to inhibit Src family kinases. PP2 treatment caused relocalisation of E-cadherin to CARGFP positive cell-cell contacts (Fig. 4F) showing that Src activity is required for CAR mediated E-cadherin localisation. However expression of CAR-GFP did not significantly alter Src activity (Fig. S3D) suggesting instead that CAR may mediate local control of Src signalling at junctions. Additionally PP2 treatment reduced localisation of CARGFP to vesicles (Fig. 4F) suggesting that internalisation of CAR and E-cadherin localisation to junctions may be linked. To investigate whether CAR could form a complex with Src, we performed GST pulldown assays with the cytoplasmic domain of CAR as well as confocal analysis of Src-GFP transiently expressed in CAR-RFP HBEC. Biochemical analysis demonstrated that Src formed a complex with the CAR cytoplasmic domain but not the GST alone control (Fig. 4G). Moreover, Src-GFP colocalised with CAR-RFP at cell-cell junctions and in vesicles, further suggesting that Src is involved in destabilisation and endocytosis of E-cadherin mediated by CAR.

CAR is phosphorylated by PKCδ. We next sought to investigate the mechanisms by which CAR controls E-cadherin dynamics. We have previously demonstrated that CAR can control intracellular signalling events in a manner dependent on the presence of the cytoplasmic domain and this results in altered cell adhesion[23]. We therefore examined whether CAR may itself be post-translationally modified within the C-terminus and whether this may in turn play a role in controlling CAR-dependent E-cadherin stability. *In silico* analysis identified two predicted PKC phosphorylation sites within the cytoplasmic tail of CAR; Thr290 and Ser293 (Fig. 5A). Indeed, analysis of CAR-GFP HBEC treated with CalyculinA to inhibit serine/threonine phosphatases revealed that CAR-GFP was phosphorylated on serine and threonine residues (Fig. S3A). Moreover, CAR-RFP and endogenous CAR in primary human epithelial cells migrated at a higher molecular weight on SDS PAGE gels following treatment with CalyculinA further suggesting a phosphorylation-dependent change in conformation of the protein (Fig. S3B and Fig. 5). Using CAR cytoplasmic domain truncation mutants (Fig. 5B[23]) we found that amino acids 261 to 315 (that contains both putative S/T PKC phosphorylation sites) were required for the induction of the higher molecular weight species of CAR following Calyculin A treatment (Fig. 5B). Using a panel of kinase inhibitors, we identified the classical and novel PKC isoforms as being required for the CalA-induced CAR band-shift (Fig. 5C).

Moreover, treatment of cells with Phorbol 12,13-dibutyrate (PDBu; an activator of cPKC's) similarly induced a higher molecular weight CAR species on SDS PAGE gels (Fig. 5C). We analysed the profile of PKC isoform expression in HBEC and demonstrated PKCδ to be the predominant cPKC expressed in these cells (data not shown). We therefore analysed whether CAR could form a complex with PKCδ using GST pulldown assays. Data revealed that PKCδ from HBEC lysates showed specific binding to GST-CAR cytoplasmic domain and this was reduced in lysates from cells treated with PDBu (Fig. 5D). Moreover, knockdown of PKCδ using siRNA significantly reduced both CalA and PDBu-induced higher molecular weight species of CAR-GFP (Fig. 5F) confirming that PKCδ is required for CAR phosphorylation. PDBu treatment of HBEC cells also resulted in recruitment of both CAR-GFP and PKCδ to cell junctions (Fig. 5E). However, CAR-GFP positive junctions showed a marked reduction in PKCδ localisation in agreement with our in vitro pulldown data, and suggesting that high levels of phosphorylated CAR leads to reduced association

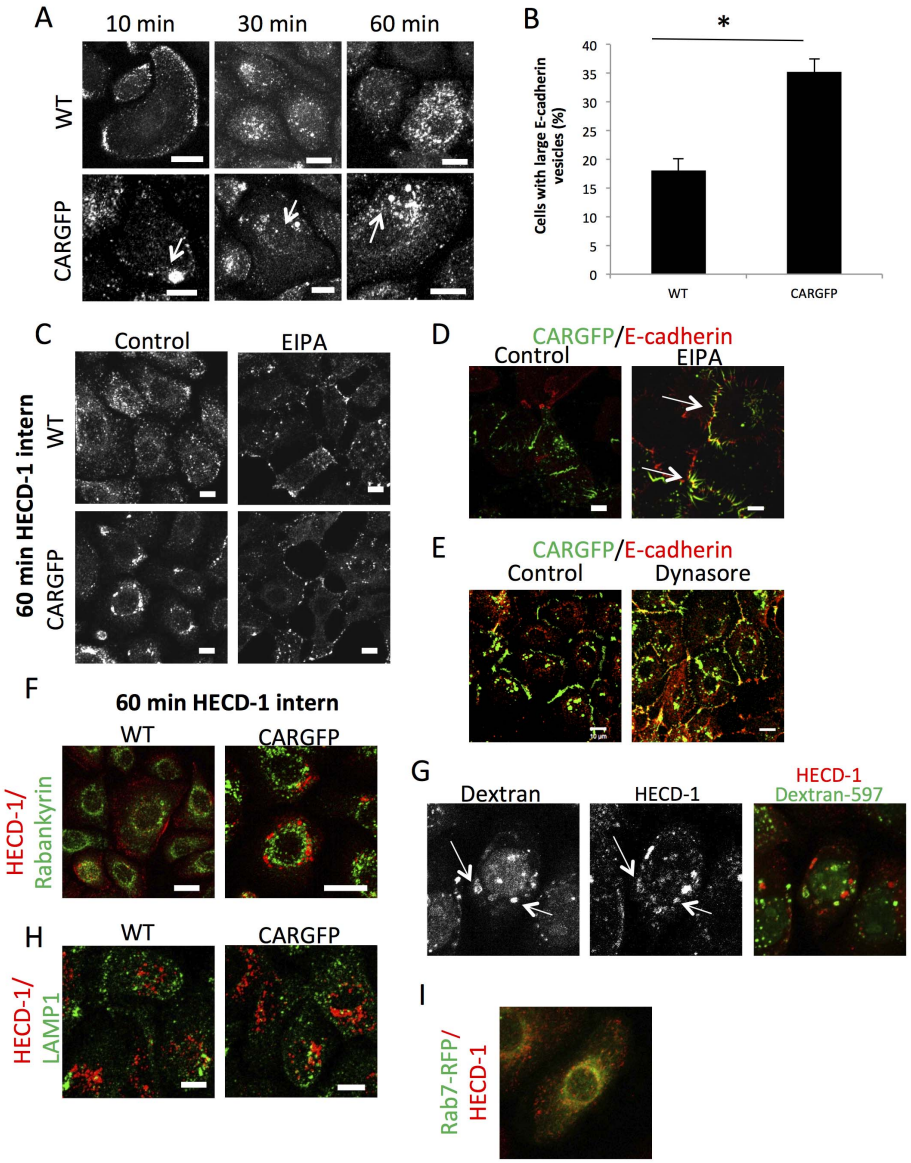

Figure 3 | CAR promotes endocytosis through a macropinocytosis-like, dynamic dependent mechanism. (A) Confocal microscopy of endocytosing E-cadherin in WT and CARGFP HBEC in HECD-1 antibody internalisation assay. Arrows highlight large E-cadherin positive vesicles. (B) Quantification of large, macropinosome-like E-cadherin containing structures observed in HECD-1 internalisation assay after 60 min of internalisation. Cells with large E-cadherin containing vesicles were counted and presented as a percentage. Images are maximum intensity projections of Z-stacks. (C) Confocal microscopy of endocytosing E-cadherin in WT and CARGFP HBEC in HECD-1 antibody internalisation assay, either untreated or treated with 100 μM EIPA for 30 min prior to addition of HECD-1 and during assay. (D) Confocal microscopy of E-cadherin in 50 : 50 mix of WT and CARGFP HBEC, either untreated or treated with 100 μM EIPA for 30 min prior to fixation. (E) Confocal microscopy of E-cadherin in DMSO control or Dynasore treated WT and CARGFP HBEC. (F) Confocal microscopy of endocytosing E-cadherin in WT and CARGFP HBEC in HECD-1 antibody internalisation assay. Cells were fixed after 60 min of HECD-1 internalisation and co-stained with anti-Rabankyrin antibody (H) or anti-LAMP1 antibody. Colocalisation is shown in yellow. (G) Confocal microscopy of endocytosing E-cadherin in CARGFP HBEC in HECD-1 internalisation assay performed in the presence of Dextran-597, and fixed after 60 min of HECD-1 internalisation. Arrow highlights colocalisation between internalised Dextran-597 and internalised HECD-1 which is shown in yellow. (I) Confocal microscopy of endocytosing E-cadherin, in Rab7-RFP expressing CARGFP HBEC, in HECD-1 antibody internalisation assay. Cells were fixed after 60 min of HECD-1 internalisation. Colocalisation between Rab7-RFP and HECD-1 is shown in yellow. Scale bars correspond to 10 μm.

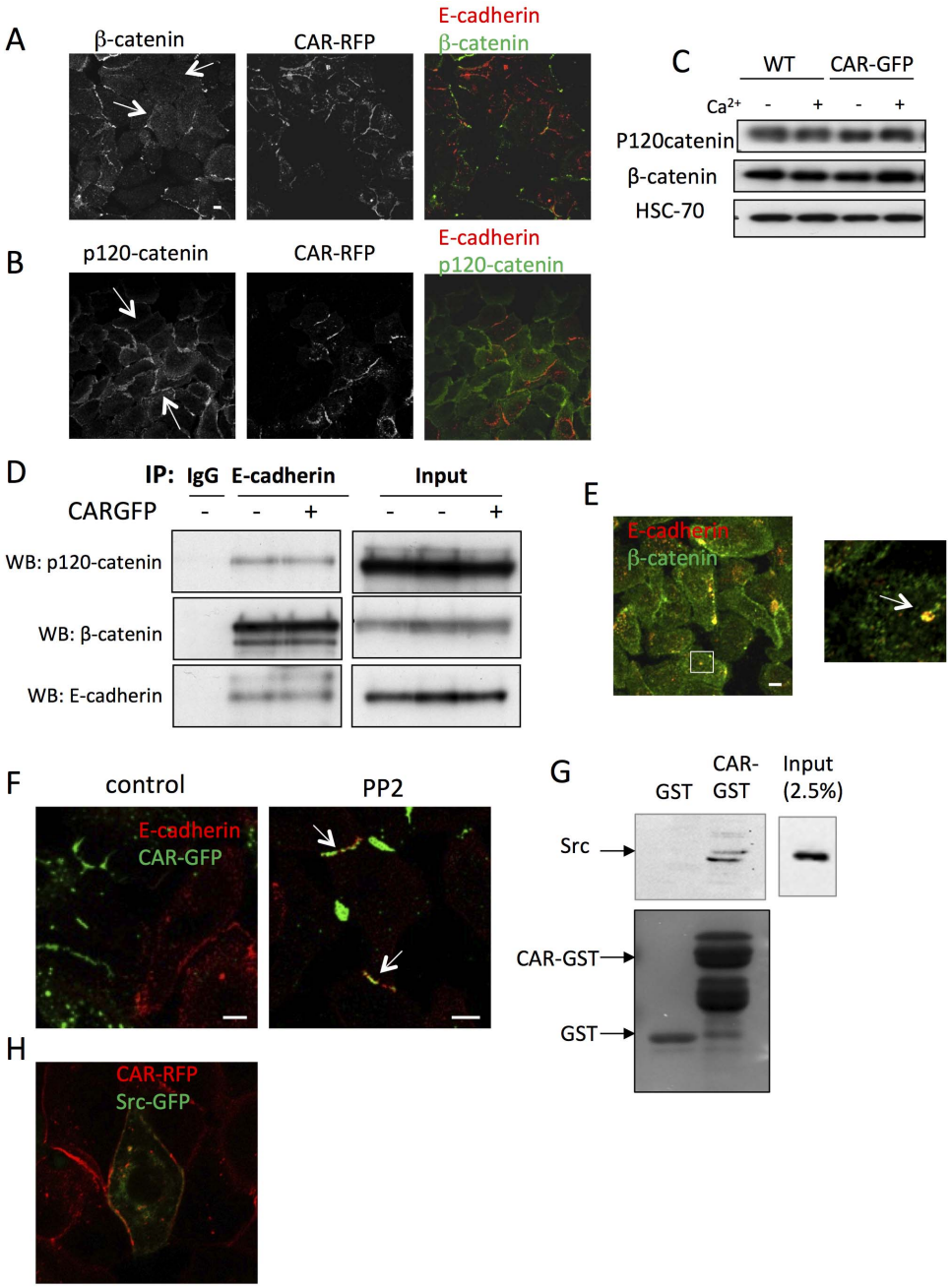

Figure 4 | CAR mediates endocytosis of E-cadherin through Src rather than disrupted binding of catenins to E-cadherin. Confocal microscopy of β-catenin (A) or p120-catenin (B) in 50:50 mix of WT and CARRFP HBEC. Arrows highlight CARRFP positive junctions. (C) WT and CARRFP HBEC lysates were separated by SDS-PAGE and analysed by immunoblotting for β-catenin, p120catenin and HSC-70 (D) E-cadherin was immunoprecipitated from wild-type and CAR-GFP-HBEC in the presence of calcium. Immunoprecipitates were separated by SDS-PAGE and analysed by immunoblotting for E-cadherin, β-catenin and p120catenin. (E) Confocal microscopy of endocytosing E-cadherin in CARGFP HBEC in HECD-1 antibody internalisation assay co-stained with anti- β-catenin antibody. Images show maximum intensity projections of z-stacks. The arrow highlights colocalisation in yellow of E-cadherin (red) and β-catenin (green) in a macropinosome-like structure. (F) Confocal microscopy of E-cadherin in 50:50 mix of WT and CARGFP HBEC, in DMSO or 1 μM PP2 treated cells. Colocalisation between E-cadherin and CAR-GFP is shown in yellow. (G) A GST-pulldown assay was carried out to investigate the interaction between CAR and Src using recombinant GST-CAR and endogenously expressed Src. Pulldown samples were probed for Src by western blotting, or gels were stained with Coumassie. Recombinant GST alone was used as a control. (H) Confocal microscopy of Src-GFP and CAR-RFP in CAR-RFP HBEC. Colocalisation between Src-GFP and CAR-RFP is shown in yellow. Scale bars correspond to 10 μm.

with PKCδ (Fig. 5E). Taken together these data suggest that PKCδ phosphorylates the cytoplasmic domain of CAR, and this potentially occurs at T290/S293 residues.

To investigate whether phosphorylation of these residues plays a role in CAR recruitment to junctions, we generated HBEC stably expressing T290/S293 phospho-mimic or non-phosphorylatable versions of CAR-GFP/RFP (DDCAR-GFP/RFP or AACAR-GFP/RFP respectively). Biochemical analysis revealed that these forms of CAR did not run as higher molecular weight species on SDS PAGE gels in cells treated with CalyculinA, confirming that these residues are required for CAR phosphorylation (Fig. 5G). Both DDCAR-GFP and AACAR-GFP localised to cell-cell junctions in

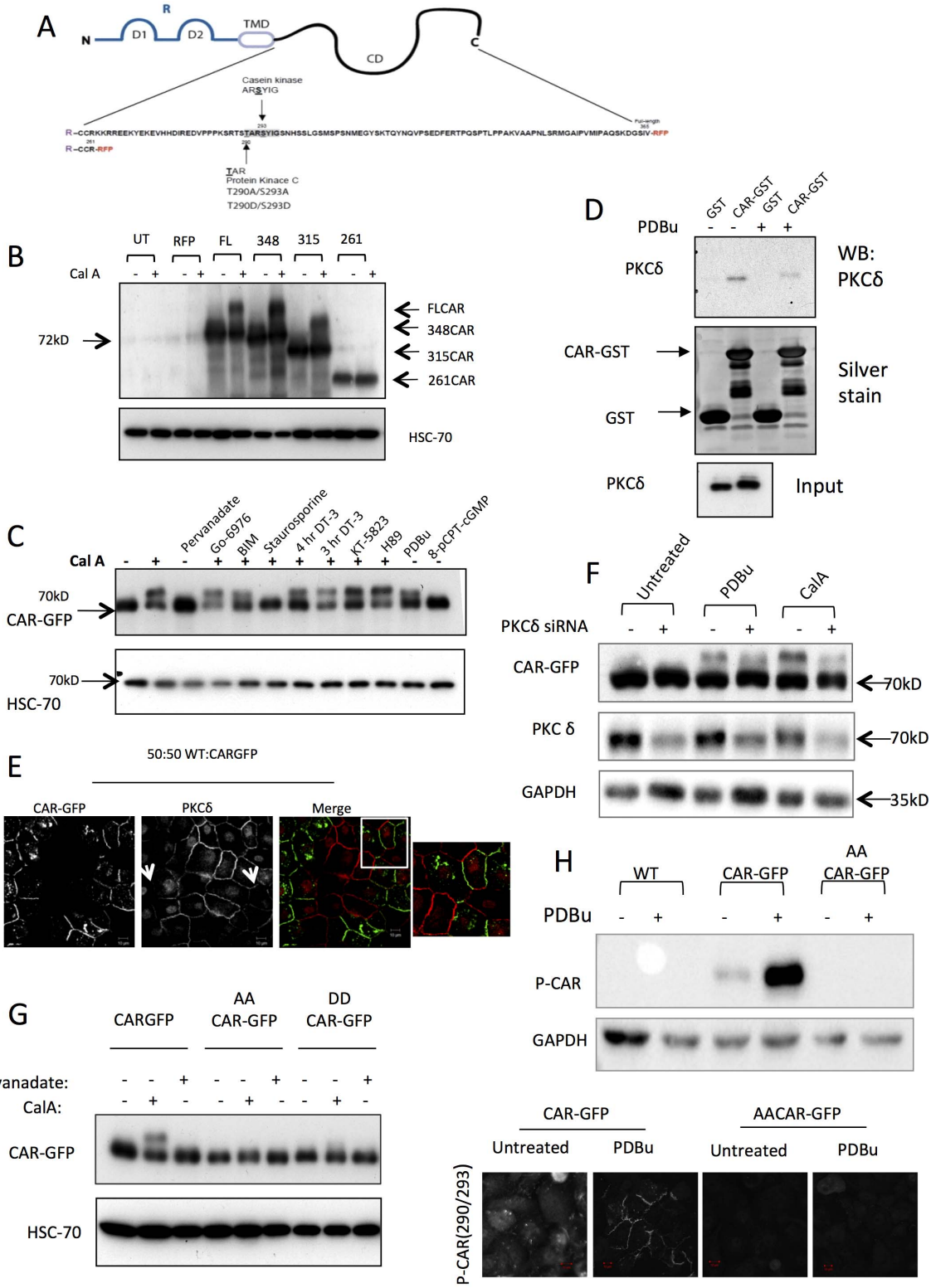

Figure 5 | CAR is ser/thr phosphorylated by PKCδ. (A) Schematic showing the cytoplasmic tail of CAR and putative phosphorylation sites. (B) Western blots of RFP tagged CAR constructs in untreated or CalA treated HBEC, probed for RFP (C) CARGFP-HBEC treated with indicated kinase inhibitors and CalA. (D) GST-pulldown assay using recombinant GST-CAR and HBEC lysates analysed by western blotting to detect PKCδ or by silver staining. Recombinant GST alone was used as a control. (E) Confocal images of a 1 : 1 mix of WT and CARGFP-HBEC treated with PDBu for 15 min before fixation and staining for PKCδ. (F) Western blot of CAR-GFP HBEC transfected with PKCδ siRNA and treated with CalA or PDBu, probed for GFP and PKCδ. (G) Western blots of HBEC expressing WT CARGFP or CAR-GFP-AA or -DD treated with CalA or Pervanadate. (H) Western blot of WT HBEC, CARGFP and AACARGFP HBEC either untreated or treated with PDBu for 15 min, probed for p-thr290/ser293-CAR (upper panel). Confocal images of CAR-GFP/AA either untreated or treated with PDBu and stained for p-thr290/ser293-CAR (lower panel). Scale bars = 10 μm.

untreated and PDBu treated samples (Fig. 6A). Interestingly, both mutant forms of CAR facilitated HBEC infection by Adenovirus serotype 5 (Ad5) to a greater degree compared with WT CAR-RFP (Fig. S3D) demonstrating dynamic control of CAR phosphorylation may play an additional role in CAR-dependent Ad5 infection. To further confirm that CAR could undergo dynamic phosphorylation, we generated a polyclonal antibody to specifically recognise CAR phosphorylated at thr290/ser293. Biochemical analysis of lysates from HBEC treated with PDBu demonstrated CAR phosphorylation specifically in CAR-GFP HBEC but not in AACAR-GFP HBEC confirming PKC-dependent phosphorylation of these sites in HBEC (Fig. 5H). Moreover, immunostaining of cells using the phosphospecific antibody revealed high levels of phosphorylated CAR-GFP at cell-cell junctions following treatment with PDBu that was not detectable in cells expressing AACAR-GFP. These data combined demonstrate that the cytoplasmic domain of CAR is phosphorylated by PKCδ and this species of CAR can be localised to epithelial cell junctions.

PKC-dependent phosphorylation of CAR mediates E-cadherin dynamics and endocytosis. In order to assess the importance of CAR phosphorylation in control of E-cadherin we first analysed E-cadherin localisation to junctions in 1 : 1 mixed cultures of WT HBEC and either CAR-GFP, AACAR-GFP or DDCAR-GFP HBEC. Interestingly, we observed that expression of AACAR but not DDCAR disrupted E-cadherin localisation to junctions (Fig. 6A) suggesting that non-phosphorylated CAR is the species that restricts CAR-mediated localisation of E-cadherin to junctions. Indeed, cells expressing DDCAR-RFP also demonstrated higher junctional mobility of E-cadherin-GFP as analysed by FRAP analysis (Fig. 6B) suggesting E-cadherin recruitment and dynamics depend on phosphorylation of CAR by PKCδ.

PKCδ has recently been shown to bind to and suppress homophillic adhesion of E-cadherin[22]. We reasoned therefore that the interaction of PKCδ with CAR and E-cadherin may act in parallel to control E-cadherin dynamics. Under homeostatic conditions, CAR did not colocalise with E-cadherin at cell-junctions. However CAR-GFP colocalised with E-cadherin during vesicle formation and early stages of E-cadherin traffic during cell-cell junction dissolution (Fig. 2C). This data and the fact that DDCAR-GFP colocalised with E-cadherin at cell-cell contacts suggested that CAR phosphorylation by PKCδ may be involved in mediating E-cadherin trafficking under basal conditions and during junction dissolution. To test this we first examined the levels and localisation of phosphorylated CAR during junction disassembly induced by calcium washout. Biochemical analysis demonstrated that total levels of phosphorylated CAR were increased 10 min after calcium washout (Fig. 6C). As previously observed (Fig. 2C), E-cadherin and CARGFP colocalised in dissolving junctions but not in stable junctions or in those undergoing early stages of cell contact dispersal (Fig. 6D). We also observed p-290/293CAR staining in a subset of E-cadherin:CAR-GFP positive intracellular vesicles (Fig. 6D, highlighted by white arrow). P-290/293CAR also localised to points of remaining cell-cell contact immediately following junction disassembly that lacked E-cadherin (Fig. 6D, highlighted by yellow arrow) demonstrating that p-CAR may control endocytosis of E-cadherin locally at these sites. To further confirm that phosphorylation of CAR by PKCδ was involved in E-cadherin trafficking we performed HECD-1 internalisation assays in WT, CAR-GFP, AACAR-GFP and DDCAR-GFP HBEC. After 60minutes, E-cadherin localised to large perinuclear macropinosome-like structures in CARGFP and AACAR-GFP, but not WT or DDCAR-GFP cells (Fig. 6E and F). Taken together, these data show that non-phosphorylated CAR mediates junctional stability and endocytosis to control levels of E-cadherin to cell-cell contacts. Since Src can be found in a complex with CAR and is important in CAR mediated relocalisation of E-cadherin, we sought to investigate whether phosphorylation of CAR by PKCδ affected the association with Src in GST pulldown assays. AACAR-GST bound at much lower levels to Src compared to the WTCAR-GST protein suggesting that this association requires CAR phosphorylation for efficient complex formation and/or maintenance. Overall this data supports a model whereby a CAR:Src complex plays a role in CAR-mediated trafficking and mobility of E-cadherin and this is in turn controlled by PKC-dependent phosphorylation of the CAR cytoplasmic domain.

Discussion

In this study we show that CAR mediates localisation of E-cadherin to cell-cell contacts by destabilising E-cadherin at junctions to promote internalisation in a Src, dynamin and macropinocytosis dependent manner. This is based on several lines of evidence; Firstly, expression of CAR-FP reduced E-cadherin at cell-cell junctions without affecting total protein expression levels or binding of p120-catenin or β-catenin to E-cadherin. Secondly, inhibitors of Src, dynamin and macropinocytosis all reversed the reduced levels of E-cadherin seen at junctions in cells overexpressing CAR. Thirdly, CAR expression reduced E-cadherin recovery at junctions, promoted uptake of the E-cadherin antibody and formation of large, E-cadherin positive, macropinosome-like endocytic structures. CAR co-immunoprecipitated with E-cadherin under low calcium culture conditions (where junction strength is low) and co-localised with E-cadherin during vesicle formation, internalisation and cell-cell adhesion disassembly. Finally, CAR mediated E-cadherin recycling was dependent on Src and was restricted following CAR phosphorylation by PKCδ. Taken together these data suggest that CAR promotes internalisation of E-cadherin through a Src and PKCδ dependent mechanism.

The specific endocytic pathway that mediates CAR-dependent endocytosis of E-cadherin remains unclear, however our data shows that both macropinocytic and dynamin-dependent mechanisms are involved. Interestingly a recent study outlined a dynamin-dependent macropincytosis-like mechanism for the internalisation of Bluetongue virus[28] suggesting that other viral receptor proteins in general may regulate multiple uptake pathways. There are conflicting reports of the involvement of dynamin in macropinocytosis[29–31], but our data raises an interesting possibility that CAR may mediate such a mechanism in order to promote internalisation of E-cadherin. However, we see significant changes in E-cadherin mobility following CAR expression, and CAR colocalises with E-cadherin specifically at sites of destabilising junctions. Therefore it seems more likely that CAR acts to destabilise E-cadherin at cell-cell contacts to promote internalisation through multiple endocytic pathways. E-cadherin containing macropinosome-like vesicles seen in CAR-GFP HBEC cells partially colocalise with LAMP1 and Rab7 suggesting that these are late endosomal compartments. However CAR mediated endocytosis of E-cadherin does not lead to degradation of E-cadherin. Thus we conclude that the internalised E-cadherin seen in CAR overexpressing cells is likely to be retained within intracellular stores or recycled back to the plasma membrane.

Colocalisation between CAR and E-cadherin is not evident in stable HBEC monolayers. However, our biochemical data suggests induction of a CARGFP:E-cadherin complex in HBEC cells maintained in media without calcium (ie: low junctional stability). Furthermore, CARGFP:E-cadherin colocalisation was seen in dissociating junctions and during vesicle formation and intracellular traffic. These data suggest that the high levels of CAR act to promote endocytosis of E-cadherin. Our discovery that CAR can be post-translationally modified through phosphorylation of Ser290/Thr293 at the C-terminus provides a potential mechanism by which this occurs. Indeed, we show that CAR-dependent E-cadherin endocytosis occurs only when T290/S293 are not phosphorylated, and phosphorylation of CAR by PKCδ results in recovery of E-cadherin

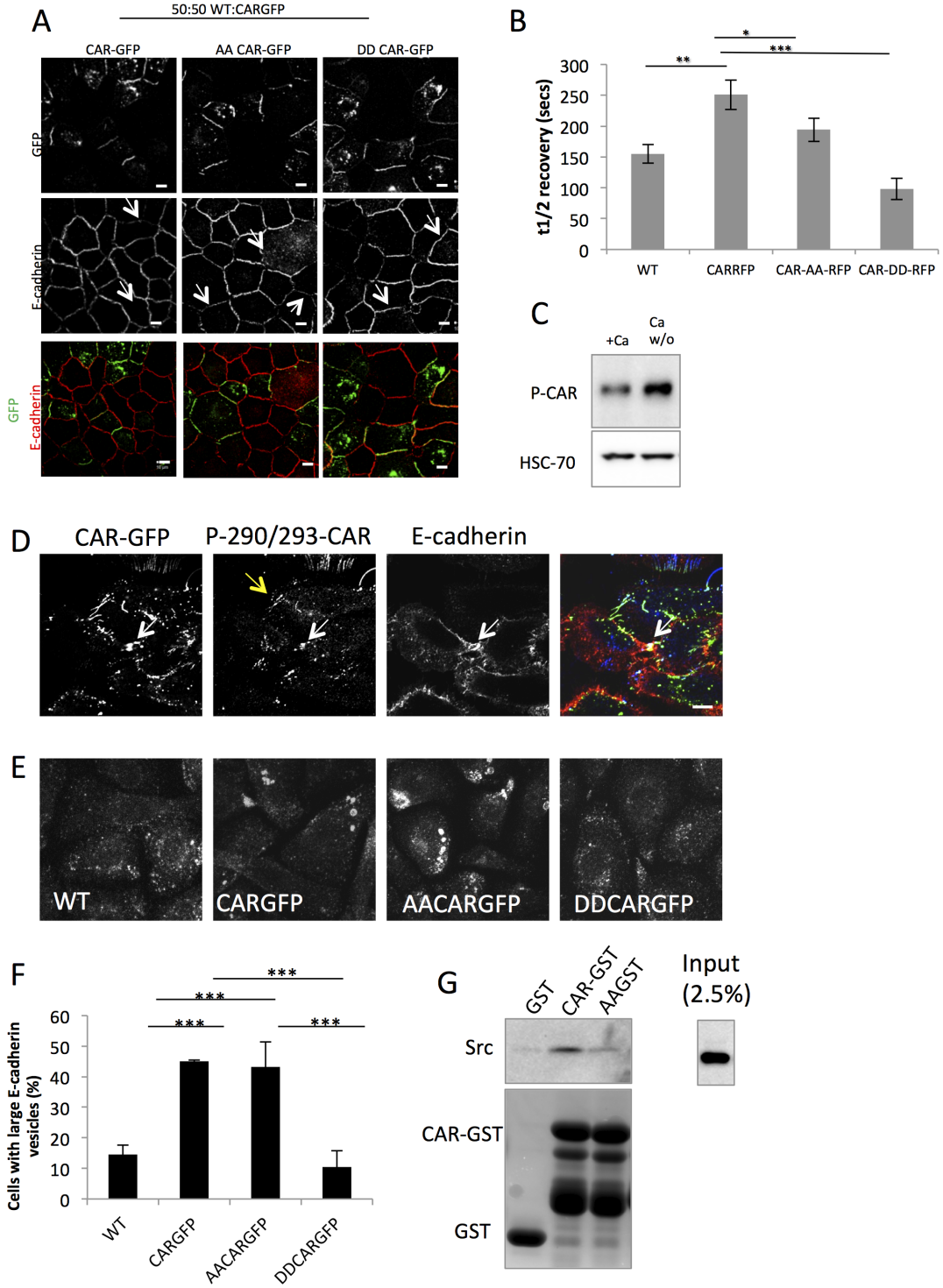

Figure 6 | CAR phosphorylation by PKCδ inhibits CAR mediated endocytosis of E-cadherin. (A) Confocal microscopy of E-cadherin and CARGFP in CARGFP, AACARGFP and DDCARGFP HBEC after 20 min PDBu stimulation. Arrows highlight CARGFP positive junctions. Co-localisation between E-cadherin and CAR-GFP is shown in yellow. (B) Analysis of E-cadherin-GFP recovery by FRAP in wild-type vs. CAR mutant expressing cells. Graphs show t1/2 recovery time. N=>25 cells for each over 3 independent experiments. (C) Western blots of CARGFP HBEC lysates grown in the presence of calcium or lysed 10 min after calcium washout, probed for p-thr290/ser293-CAR or HSC-70 as loading control. (D) Confocal microscopy of p-thr290/ser293-CAR, E-cadherin and CARGFP 10 min after calcium washout. White arrow highlights a dissociating junction positively stained for p-CAR and E-cadherin. Yellow arrow highlights p-CAR positive cell-cell contact after E-cadherin/junction dispersal. (E) Maximum intensity projections of confocal z-stacks of WT, CARGFP, AACARGFP and DDCARGFP HBEC in HECD-1 antibody internalisation assay after 60 min of antibody internalisation. (F) Quantification of large, macropinosome-like E-cadherin containing structures observed in HECD-1 internalisation assay after 60 min of internalisation in WT, CARGFP, AACARGFP and DDCARGFP HBEC. Images presented in E were used to quantify the number of cells with macropinosome-like structures. More than 100 cells per condition were counted and presented as a percentage of the total number of cells. (E) A GST-pulldown assay was carried out to investigate the interaction between CAR and Src using recombinant GST-CAR or GST-AACAR and endogenously expressed Src. Pulldown samples were probed for Src by western blotting, or gels were stained with Coumassie. Recombinant GST alone was used as a control. Error bars are SEM. * = $p < 0.05$, ** = $p < 0.01$ *** = $p < 0.005$. Scale bars correspond to 10 μm.

levels at cell-cell junctions. This suggests that CAR phosphorylation has a protective effect on E-cadherin junctional localisation and perhaps serves to slow endocytosis of E-cadherin. Our confocal analysis revealed that CAR is phosphorylated during dissociation of adherens junctions immediately prior to endocytosis of E-cadherin and remains within the membrane at these sites even after the junction has entirely separated. Additionally, CAR-phosphorylation increased after calcium washout suggesting that CAR phosphorylation occurs during dissociation of cell-cell contacts, and may act to slow down or even prevent this process.

Phosphorylation of CAR by PKCδ is an important component in CAR-mediated E-cadherin localisation and dynamics. However PKCδ has also been previously shown to play a direct role in controlling E-cadherin behaviour. PKCδ interacts directly with E-cadherin to suppress homodimerisation and to promote HGF[22] and EGF[32] mediated cell scattering. PKCδ activity can trigger phosphatase dependent serine de-phosphorylation of p120-catenin to reduce its localisation to cell-cell junctions[33] and can also lead to downregulatation of the cadherin:catenin complex[33]. However our data shows that treatment of HBEC with PDBu to activate PKC causes increased E-cadherin at cell junctions unless CAR is overexpressed. This suggests that PKCδ may require CAR to facilitate loss of E-cadherin from junctions. PKCδ binds directly to CAR and dissociates after PDBu treatment, although it is not yet clear whether PKCδ activity or the resulting CAR phosphorylation event is responsible for complex dissociation. Further analysis will be required in live cells to define the dynamic nature of this complex.

PKCδ can act downstream of Src to promote E-cadherin endocytosis[33]. Here we show that CAR can associate with Src, and that Src activity is required for CAR-dependent movement of E-cadherin away from cell-cell junctions. Whether PKCδ is downstream of Src in this pathway remains to be investigated. Src kinase is known to exert both positive and negative influences on E-cadherin and adherens junction proteins, as well as play a role in macropinocytosis[20,34,35]. Src can control E-cadherin dynamics in a number of ways, however the classic role for Src in E-cadherin endocytosis is through phosphorylation of E-cadherin which promotes ubiquitination of E-cadherin by Hakai[36]. This involves dissociation of p120-catenin from E-cadherin which would otherwise block binding of Hakai. Our data show that whilst a pool of p120-catenin remains at cell-cell contacts in CAR overexpressing cells, CAR expression does not affect interaction of E-cadherin with either β-catenin or p120-catenin. Since CAR does not drive dissociation of p120-catenin from E-cadherin, Src is therefore unlikely to be driving the ubiquitination of E-cadherin under these conditions. How Src mediates CAR dependent E-cadherin localisation therefore remains to be determined. In addition to this, our data shows that CAR dependent endocytosis of E-cadherin leads to recycling rather than degradation of E-cadherin. Preservation of both E-cadherin:catenin interactions would direct endocytosed E-cadherin towards recycling pathways: binding of p120-catenin blocks binding of Hakai[36,37], while β-catenin directs E-cadherin to the exocytosis pathway through interaction with the exocyst complex (Langevin et al., 2005). Taken together these data substantiate our hypothesis that CAR promotes recycling of E-cadherin, and further suggest that CAR, Src and PKCδ may act together as a complex to control E-cadherin dynamics in a CAR-phosphorylation dependent manner.

The formation of adherens junctions occurs early during cell-cell contact and subsequent tight junction assembly is thought to promote redistribution of adherens junction components and thus a polarised epithelium[38]. Tight junctions regulate lateral diffusion/migration of basolateral adhesion proteins in polarised epithelia. Consistent with this idea, our FRAP analysis of E-cadherin demonstrated reduced lateral diffusion in CAR overexpressing cells compared to control HBEC. E-cadherin shows reduced lateral diffusion in mature compared with immature junctions[15] and in the latter, redistribution of E-cadherin is mainly due to dynamin-dependent endocytosis/exocytosis mechanisms[15,38]. Since CAR acts to restrict mobility of E-cadherin and promote dynamin-dependent recycling rather than degradation, it is possible that CAR also influences polarisation of epithelia through maturation of epithelial junctions. In fact, CAR expression levels have been shown to vary in cells grown in 2D or 3D culture, and on cell confluence in 2D culture in breast epithelial cells (Anders et al., 2003) suggesting a link between CAR and polarised epithelial architecture. Our own studies have linked the cytoplasmic tail of CAR to the role of CAR in signalling to integrins and cell-matrix adhesion[23] both of which are essential for maintenance of polarised epithelium. It will be interesting in future studies to determine the effect of CAR expression and phosphorylation on epithelial polarity.

Phosphorylation of CAR has not been previously reported and raises the possibility that dynamic phosphorylation of CAR may be important in other CAR-dependent processes. CAR has recently been shown to be important for trans-epithelial migration (TEM) of neutrophils and γδ-T cells[39,40]. In endothelial cells endocytosis of VE-cadherin is important for trans-migration of leukocytes. This raises the intriguing possibility that CAR phosphorylation may be important in TEM either through modulation of E-cadherin endocytosis or via an alternate mechanism. We have also previously shown that the cytoplasmic tail of CAR is not necessary for Ad5 infection[23]. In fact, data presented here show that prevention of dynamic phosphorylation of CAR increases Ad5eGFP transduction in HBEC. These data suggest that CAR phosphorylation may be involved in cell-cell and cell-matrix adhesion as well as Ad5 infection. Several studies have reported altered CAR expression levels as well as roles for CAR in tumour cell progression, although these studies report both pro-and anti-progression properties for CAR[9–11,41–45]. Specifically, CAR has been associated with both loss and increases in E-cadherin expression and localisation in lung cancer[10] and in oral squamous carcinoma[11]. Whether CAR plays a key role in tumourigenesis remains to be investigated; our data presented here suggest potential mechanisms by which CAR, via its aberrant phosphorylation, could influence tumourigenesis through modulation of E-cadherin at cell junctions and also potentially through control of integrin activation and cell-matrix adhesion[23]. CAR is traditionally known as a receptor for adenovirus and a component of tight junctions. We do not see an effect of CAR expression on tight junction formation in our HBEC model, as measured by permeability assays, however CAR clearly has a role to play in tight junctions in other tissues particularly in the heart[6] and in lymph vessels[5]. Thus phosphorylation of CAR by PKCδ could be important for dynamic control of cell permeability in these and other cell types.

In summary our data support a model whereby phosphorylation of CAR controls E-cadherin dynamics through Src and dynamin-dependent endocytosis. De-phosphorylated CAR acts to prevent E-cadherin localisation to junctions through promotion of recycling, PKCδ dependent phosphorylation of CAR maintains E-cadherin at junctions and may serve to stabilise cell-cell adhesion in the epithelium.

Methods

Cell culture. Immortalised human bronchial epithelial cells (HBEC) were a gift from Dr Jerry Shay (UT Southwestern[46]) and were grown in KSFM (Invitrogen). Primary human tracheal epithelial cells (HTEpC-c) were obtained from Promocell and were grown in Airway Epithelial Cell Growth Medium (Promocell). All CAR expressing stable cell lines were produced using lentiviral expression. Lentivirus particles were generated in 293T packaging cells (as in[47]) and these cells were maintained in DMEM containing 10% FCS, supplemented with glutamine.

Antibodies and reagents. Anti-phospho-serine, anti-phosho-threonine, anti-phospho-tyrosine were from Cell Signalling Technology. Anti-E-cadherin (HECD-1) and anti-ZO-1 antibodies were from Invitrogen. Anti-Rabankyrin antibody was from Thermofischer. Anti- Rab11, EEA1, and LAMP1 were from Cell signalling Technology. Anti-CAR (H300), anti-β-catenin and anti-PKCδ antibodies were from Santa Cruz. Anti-p120catenin was from BD biosciences and anti-RFP and anti-Rab5

were from Abcam. Anti-mouse HRP and anti-rabbit-HRP were from DAKO, anti-mouse-568, anti-rabbit-568 and phalloidin-633 were all obtained from Invitrogen. CalyculinA, Sodium orthovanadate, Gö6976, BIM, Staurosporine, DT-3, KT-5823 and Phorbol-12,13-dibutyrate (PDBu) were obtained from Calbiochem. 8-pCPT-cGMP (PKG activator), H89 (PKA inhibitor) EIPA, PP2, PP3 and dynasore were obtained from Sigma-Aldrich. Ad5eGFP is E1-E3 deleted, replication deficient recombinant adenovirus type 5 that expresses green fluorescent protein under the control of the cytomegalovirus promoter (Baylor College of Medicine). Ad5FK was produced and purified as previously described[48]. p-CARthr290/ser293 polyclonal antibody was developed by Perbioscience (Thermofisher) using the peptide Ac-RTS(pT)AR(pS)YIGSNH-C and was affinity purified before use.

Plasmids. Plasmids encoding full-length CAR and deletion mutants have been described previously[23]. Full length CAR was cloned in frame into pHR9SIN-SEW lentiviral expression vector, which was a gift from Dr Adrian Thrasher (Institute of Child Health, UCL, London[47];), and into pGEX-2T. Full length and mutant CAR sequences were cloned pHR9SIN-SEW lentiviral expression plasmid and shRNA sequences (hairpin sequence for shA6 TGCTGTTGACAGTGAGCGCTG GAAGTGACTTTAAGATAAATAGTGAAGCCACAGATGTA) were obtained from Open Biosystems (Thermofisher) in the pGIPZ expression plasmid. Phospho-mutant constructs were generated using site directed mutagenesis. The sequences of oligonucleotides used are available on request. The Rab7-RFP plasmid was a kind gift from Dr Mark Dodding (Randall Division, KCL, London).

Confocal microscopy. Cultured cells were washed with PBS, fixed with 4% PFA in PBS for 10 min and permeabilised with 0.2% TritonX-100 for 10 min. Cells were incubated with primary antibodies for 2 hours and appropriate secondary antibodies conjugated to Alexafluo-568 or cy5 and Phalloidin conjugated to Alexafluor 568 or 633 for 1 hour. Cells were mounted onto slides using Immunofluore (ICN). Confocal microscopy of HBEC alone was performed using an LSM510 using a 63 × oil objective and excitation wavelengths of 488 nm (for GFP or Alexafluor-488), 543 nm (for Alexafluor-568) and 633 nm (for Alexafluor-633 and cy5). Confocal microscopy of THP-1 cells binding to HBEC was performed using a Nikon A1R confocal microscope.

E-cadherin endocytosis assay. Cells were incubated for 1 h at 4°C with 1 μg/ml HECD-1 diluted in optimem. Coverslips (or cultures) were washed with ice-cold PBS to remove the unbound antibody and the media was replaced with KSFM pre-warmed to 37°C. After incubation at 37°C for varying periods of time (0–60 mins), cells were then washed with PBS and returned to 4°C. The residual surface-bound antibody was removed by acid washing (0.5 M acetic acid, 0.5 M NaCl; 3 × 5 min washes). Cells were washed with PBS before either fixation with 4% paraformaldehyde for immunofluorescence. To quantify HECD-1 internalisation the HECD-1 intensity per cell was analysed in cells fixed without antibody internalisation at 37°C and without stripping to obtain the intensity value for externally bound antibody. This was then used to normalise the internalised HECD-1 intensity after 60 min of internalisation at 37°C and acid stripping using the following equation:

$$\%\ \text{HECD-1 internalisation} = \{\text{HECD-1 intensity of 60min (acidstripped)}/\text{HECD-1 intensity of 0min(unstripped)}\} * 100$$

More than 60 cells per condition were analysed per experiment.

Widefield microscopy. Cultured cells were washed with PBS, fixed with 4% PFA in PBS for 10 min and permeabilised with 0.2%triton for 10 min. Cells were incubated with primary antibodies for 2 hours and appropriate secondary antibodies conjugated to alexafluo-568 or cy5 and phalloidin conjugated to Alexafluor 568 or 633 for 1 hour. Cells were mounted onto slides using FluorSave (Calbiochem). Widefield microscopy was performed using an Olympus IX81 microscope. 5 × 5 tile-scans were obtained using a 10 × air objective using identical camera acquisition times and initial analysis to knit the tiles together was performed using Metamorph software. Tiffs created using Metamorph were then used in Image J to quantify E-cadherin signal intensity at cell junctions. More than 100 junctions per condition were analysed and averaged.

Western blotting. 100,000 HBEC per condition were cultured either in normal growth media or in media supplemented with 0.1 g/L calcium nitrate for 24 hours before lysis in 100 ul sample buffer containing β-mercaptoethanol at room temperature. Lysates were immediately subjected to SDS-PAGE and blotted using nitrocellulose membrane. Blots were blocked and probed using 3% milk/PBS-0.2%tween or 5%BSA/TBS-0.1%tween.

Sample preparation for CARGFP band-shift assay. CARGFP HBEC cells were cultured to confluency in normal growth media before treatment with the following protein kinase inhibitors and activators. Calyculin A (300 nM 15 min), PDBu (1 μM 20 min) and 8-pCPT-cGMP (50 μM). Where indicated, cells were pre-treated for 90 min unless otherwise stated with the following kinase inhibitors; Gö6976 (1 μM), BIM (10 μM), Staurosporine (1 μM), DT-3 (50 μM), KT5823 (1 μM) and H89 (1 μM). Cells were then lysed and analysed as described in the previous paragraph.

Co-immunoprecipitation. HBEC and CAR-GFP-HBEC were cultured either in normal growth media or in media supplemented with 0.1 g/L calcium nitrate for 24 hours before lysis in IP lysis buffer (pH7.4 50 mM Tris, 150 mM NaCl, 1 mM EDTA, 1% Triton, 1% NP40, PI cocktail). Lysates were incubated with 5 μg E-cadherin (HECD-1) antibodies pre-bound to A/G agarose beads overnight before washing the beads with 1 ml IP lysis buffer 3 times immunocomplexes were separated using SDS-PAGE and immunoblotted for either E-cadherin, β-catenin or GFP (for CAR-GFP).

***In vitro* pulldown assay.** GST-fusion constructs were expressed in *E. coli* BL21 competent cells using conditions recommended by the manufacturer (Amersham Pharmacia Biotech). Pulldown assays using CAR-GST were carried out using wild-type HBEC lysed in IP lysis buffer and incubated with GST or CAR-GST attached to glutathione beads overnight. Beads were washed three times with IP lysis buffer and complexes were separated using SDS-PAGE.

Fluorescence activated cell sorting (FACS). Ad5GFP was added to confluent monolayers of cells at 100 or 5000 pfu/cell for three minutes at 37°C. Unattached virus was removed by washing three times with warm PBS. The cell monolayers were then covered with pre-warmed growth media. The cells were then transferred to a cell incubator at 37°C for 18 hours and then processed for GFP expression. After 18 hours adherent cells were harvested with trypsin/EDTA (Gibco) at 37°C. The cells were centrifuged at 200 g for 5 minutes and the supernatant removed. Cells were fixed in 1% PFA on ice washed, with FACSFlow and analysed using a BD FACSCalibur flow cytometer (BD Biosciences). Quadrant markers were set based upon background fluorescence from uninfected cells.

Fluorescence recovery activated photobleaching (FRAP). HBEC and CAR-RFP-HBEC were transiently transfected in 6 well plates with E-cadherin-GFP for 48 hours before before addition of calcium containing medium. Junctions expressing E-cadherin-GFP were identified using an Eclipse Ti-E confocal microscope (Nikon Instruments) and small sections of the junctions were selected. 5 images were taken of the selected area every 15 seconds followed by bleaching using 65 iterations (at 488 nm) to ensure all the GFP in the region of interest had been bleached. Further imaging every 15 seconds for another 7 minutes to monitor the fluorescence recovery then followed this. Images obtained were then examined using Image J and the rate of recovery was calculated taking into account the fading of fluorescence over time. Fading was corrected with the following equation -

$$= \text{Intensity of Region of interest}/\text{Intensity of whole image}$$

Percentage rate of recovery was calculated using the equation.

$$= \text{Corrected Value (for each time point)}/\text{Av of corrected pre-bleached values} \times 100$$

Statistics. Results are expressed as the mean ± s.e.m. from the specified number of experiments, as indicated in the figure legends. Student's t-test was used to analyse statistical significance.

1. Wirtz-Peitz, F. & Zallen, J. A. Junctional trafficking and epithelial morphogenesis. *Curr Opin Genet Dev* **19**, 350–356 (2009).
2. Coyne, C. B. & Bergelson, J. M. CAR: a virus receptor within the tight junction. *Adv Drug Deliv Rev* **57**, 869–882 (2005).
3. Cohen, C. J. *et al.* The coxsackievirus and adenovirus receptor is a transmembrane component of the tight junction. *Proc Natl Acad Sci U S A* **98**, 15191–15196 (2001).
4. Vigl, B. *et al.* Coxsackie- and adenovirus receptor (CAR) is expressed in lymphatic vessels in human skin and affects lymphatic endothelial cell function in vitro. *Exp Cell Res* **315**, 336–347 (2009).
5. Mirza, M. *et al.* Essential role of the coxsackie- and adenovirus receptor (CAR) in development of the lymphatic system in mice. *PLoS One* **7**, e37523 (2012).
6. Pazirandeh, A. *et al.* Multiple phenotypes in adult mice following inactivation of the Coxsackievirus and Adenovirus Receptor (Car) gene. *PLoS One* **6**, e20203 (2011).
7. Hussain, F. *et al.* CAR modulates E-cadherin dynamics in the presence of adenovirus type 5. *PLoS One* **6**, e23056 (2011).
8. Chen, Z. *et al.* Expression of the coxsackie and adenovirus receptor in human lung cancers. *Tumour Biol* **34**, 17–24 (2013).
9. Matsumoto, K., Shariat, S. F., Ayala, G. E., Rauen, K. A. & Lerner, S. P. Loss of coxsackie and adenovirus receptor expression is associated with features of aggressive bladder cancer. *Urology* **66**, 441–446 (2005).
10. Veena, M. S., Qin, M., Andersson, A., Sharma, S. & Batra, R. K. CAR mediates efficient tumor engraftment of mesenchymal type lung cancer cells. *Lab Invest* **89**, 875–886 (2009).
11. Saito, K. *et al.* Coxsackie and adenovirus receptor is a critical regulator for the survival and growth of oral squamous carcinoma cells. *Oncogene* (2013). doi: 10.1038/onc.2013.66.
12. de Beco, S., Amblard, F. & Coscoy, S. New insights into the regulation of E-cadherin distribution by endocytosis. *Int Rev Cell Mol Biol* **295**, 63–108 (2012).

13. Baum, B. & Georgiou, M. Dynamics of adherens junctions in epithelial establishment, maintenance, and remodeling. *J Cell Biol* **192**, 907–917 (2011).
14. Bryant, D. M. & Stow, J. L. The ins and outs of E-cadherin trafficking. *Trends Cell Biol* **14**, 427–434 (2004).
15. de Beco, S., Gueudry, C., Amblard, F. & Coscoy, S. Endocytosis is required for E-cadherin redistribution at mature adherens junctions. *Proc Natl Acad Sci U S A* **106**, 7010–7015 (2009).
16. Le, T. L., Joseph, S. R., Yap, A. S. & Stow, J. L. Protein kinase C regulates endocytosis and recycling of E-cadherin. *Am J Physiol Cell Physiol* **283**, C489–499 (2002).
17. Paterson, A. D., Parton, R. G., Ferguson, C., Stow, J. L. & Yap, A. S. Characterization of E-cadherin endocytosis in isolated MCF-7 and chinese hamster ovary cells: the initial fate of unbound E-cadherin. *J Biol Chem* **278**, 21050–21057 (2003).
18. Bryant, D. M. *et al.* EGF induces macropinocytosis and SNX1-modulated recycling of E-cadherin. *J Cell Sci* **120**, 1818–1828 (2007).
19. Swaminathan, G. & Cartwright, C. A. Rack1 promotes epithelial cell-cell adhesion by regulating E-cadherin endocytosis. *Oncogene* **31**, 376–389 (2012).
20. Mettlen, M. *et al.* Src triggers circular ruffling and macropinocytosis at the apical surface of polarized MDCK cells. *Traffic* **7**, 589–603 (2006).
21. Solis, G. P. *et al.* Reggies/flotillins regulate E-cadherin-mediated cell contact formation by affecting EGFR trafficking. *Mol Biol Cell* **23**, 1812–1825 (2012).
22. Chen, C. L. & Chen, H. C. Functional suppression of E-cadherin by protein kinase Cdelta. *J Cell Sci* **122**, 513–523 (2009).
23. Farmer, C., Morton, P. E., Snippe, M., Santis, G. & Parsons, M. Coxsackie adenovirus receptor (CAR) regulates integrin function through activation of p44/42 MAPK. *Exp Cell Res* **315**, 2637–2647 (2009).
24. Kerr, M. C. & Teasdale, R. D. Defining macropinocytosis. *Traffic* **10**, 364–371 (2009).
25. Masereel, B., Pochet, L. & Laeckmann, D. An overview of inhibitors of Na(+)/H(+) exchanger. *Eur J Med Chem* **38**, 547–554 (2003).
26. Nelson, W. J. & Nusse, R. Convergence of Wnt, beta-catenin, and cadherin pathways. *Science* **303**, 1483–1487 (2004).
27. Ishiyama, N. *et al.* Dynamic and static interactions between p120 catenin and E-cadherin regulate the stability of cell-cell adhesion. *Cell* **141**, 117–128 (2010).
28. Gold, S., Monaghan, P., Mertens, P. & Jackson, T. A clathrin independent macropinocytosis-like entry mechanism used by bluetongue virus-1 during infection of BHK cells. *PLoS One* **5**, e11360 (2010).
29. Cao, H., Chen, J., Awoniyi, M., Henley, J. R. & McNiven, M. A. Dynamin 2 mediates fluid-phase micropinocytosis in epithelial cells. *J Cell Sci* **120**, 4167–4177 (2007).
30. Meier, O. *et al.* Adenovirus triggers macropinocytosis and endosomal leakage together with its clathrin-mediated uptake. *J Cell Biol* **158**, 1119–1131 (2002).
31. Schlunck, G. *et al.* Modulation of Rac localization and function by dynamin. *Mol Biol Cell* **15**, 256–267 (2004).
32. Singh, R., Lei, P. & Andreadis, S. T. PKC-delta binds to E-cadherin and mediates EGF-induced cell scattering. *Exp Cell Res* **315**, 2899–2913 (2009).
33. Chen, Y. *et al.* Acidic extracellular pH induces p120-catenin-mediated disruption of adherens junctions via the Src kinase-PKCdelta pathway. *FEBS Lett* **585**, 705–710 (2011).
34. McLachlan, R. W., Kraemer, A., Helwani, F. M., Kovacs, E. M. & Yap, A. S. E-cadherin adhesion activates c-Src signaling at cell-cell contacts. *Mol Biol Cell* **18**, 3214–3223 (2007).
35. Kasahara, K. *et al.* Role of Src-family kinases in formation and trafficking of macropinosomes. *J Cell Physiol* **211**, 220–232 (2007).
36. Fujita, Y. *et al.* Hakai, a c-Cbl-like protein, ubiquitinates and induces endocytosis of the E-cadherin complex. *Nat Cell Biol* **4**, 222–231 (2002).
37. Xiao, K. *et al.* p120-Catenin regulates clathrin-dependent endocytosis of VE-cadherin. *Mol Biol Cell* **16**, 5141–5151 (2005).
38. Huang, J. *et al.* Differential regulation of adherens junction dynamics during apical-basal polarization. *J Cell Sci* **124**, 4001–4013 (2011).
39. Verdino, P., Witherden, D. A., Havran, W. L. & Wilson, I. A. The molecular interaction of CAR and JAML recruits the central cell signal transducer PI3K. *Science* **329**, 1210–1214 (2010).
40. Witherden, D. A. *et al.* The junctional adhesion molecule JAML is a costimulatory receptor for epithelial gammadelta T cell activation. *Science* **329**, 1205–1210 (2010).
41. Yamashita, M., Ino, A., Kawabata, K., Sakurai, F. & Mizuguchi, H. Expression of coxsackie and adenovirus receptor reduces the lung metastatic potential of murine tumor cells. *Int J Cancer* **121**, 1690–1696 (2007).
42. Stecker, K. *et al.* Impact of the coxsackievirus and adenovirus receptor on the adenoma-carcinoma sequence of colon cancer. *Br J Cancer* **104**, 1426–1433 (2011).
43. Okegawa, T. *et al.* The dual impact of coxsackie and adenovirus receptor expression on human prostate cancer gene therapy. *Cancer Res* **60**, 5031–5036 (2000).
44. Qin, M., Escuadro, B., Dohadwala, M., Sharma, S. & Batra, R. K. A novel role for the coxsackie adenovirus receptor in mediating tumor formation by lung cancer cells. *Cancer Res* **64**, 6377–6380 (2004).
45. Korn, W. M. *et al.* Expression of the coxsackievirus- and adenovirus receptor in gastrointestinal cancer correlates with tumor differentiation. *Cancer Gene Ther* **13**, 792–797 (2006).
46. Ramirez, R. D. *et al.* Immortalization of human bronchial epithelial cells in the absence of viral oncoproteins. *Cancer Res* **64**, 9027–9034 (2004).
47. Demaison, C. *et al.* High-level transduction and gene expression in hematopoietic repopulating cells using a human immunodeficiency [correction of imunodeficiency] virus type 1-based lentiviral vector containing an internal spleen focus forming virus promoter. *Hum Gene Ther* **13**, 803–813 (2002).
48. Kirby, I. *et al.* Mutations in the DG loop of adenovirus type 5 fiber knob protein abolish high-affinity binding to its cellular receptor CAR. *J Virol* **73**, 9508–9514 (1999).

Acknowledgements

This work was funded by a Royal Society University Research Fellowship (to MP), Medical Research Council grant (to GS), Science and Facilities Research Council (to GS) and the National Institute of Health Research Comprehensive Biomedical Research Centre at Guy's & St Thomas' Trust (to GS).

Author contributions

Experiments and data analysis were performed by P.E.M., A.H., T.N. and M.P. with input from G.S. M.P. and G.S. devised the original study with input from P.E.M. P.E.M. and M.P. wrote the manuscript with input from G.S.

Additional information

Supplementary information accompanies this paper at http://www.nature.com/scientificreports

Competing financial interests: The authors declare no competing financial interests.

How to cite this article: Morton, P.E., Hicks, A., Nastos, T., Santis, G. & Parsons, M. CAR regulates epithelial cell junction stability through control of E-cadherin trafficking. *Sci. Rep.* **3**, 2889; DOI:10.1038/srep02889 (2013).